



INFLUENCE OF MICROSTRUCTURE, PRODUCED BY HEAT TREATMENT AND SEVERE PLASTIC DEFORMATION, ON TRIBOLOGICAL PROPERTIES OF LOW-CARBON STEEL

V.I. Semenov¹, Song-Jeng Huang², L.Sh. Shuster³, Po-Chou Lin⁴

^{1,3}Ufa State Aviation Technical University, Ufa, Russia, semenov-vi@rambler.ru

^{2,4}National Chung Cheng University, Taiwan, ROC, imehsj@gmail.com

Abstract: This paper presents the results of tribological investigations conducted on steel 20 with the carbon content of up to 0.2%. The steel was studied in the three conditions: initial (hot-rolled), after heat-treatment (quenching+tempering) and after heat treatment with subsequent severe plastic deformation (SPD) performed by equal channel angular pressing technique (ECAP). It was stated that after various treatments the material acquires various structural conditions and possesses various strength properties and has a considerable difference in oxygen content in the surface layer. This influences the tribological properties during the contact with tool steel. The lowest values of adhesive bond shear strength, friction coefficient and wear rate are demonstrated in the material after martempering with subsequent SPD by ECAP technique. The surface of the investigated material after SPD treatment by the ECAP technique possesses a highest bearing capacity and requires more time for wearing-in in friction assemblies. Oxygen content increase in the form of metal oxides on the surface of low-carbon steels is accompanied by a decrease of the adhesive component of friction coefficient.

Keywords: Severe plastic deformation; adhesive bond shear strength; low-carbon steel; friction coefficient; wear rate; microstructure.

1. INTRODUCTION

It is known that harder materials provide lower wear rate and friction coefficient [1]. There are various ways to enhance hardness of alloys by heat treatment [2, 3]. However, heat treatment may be an inefficient way to enhance hardness of many pure metals and low-carbon alloys. For such materials, various thermochemical [4-6] and surface plastic treatments [5-7] are used to enhance the strength of the surface of the materials under processing. The disadvantage of these techniques is that they results in a considerably shallow depth of the strengthened surface layer; that is why they may be used only for final treatment or for relatively simple and low-loaded parts in tribological pairs.

There are known papers on evaluation of the influence of microstructure and phase compositions of tool carbon steel on its tribological properties [5, 6, 8-10]. There tribological investigations were conducted on materials subjected to various

treatments, which led to the changes of microstructure and phase composition of the materials.

Recently, the technology of effective and multiple strength enhancements retaining high technological plasticity, based on severe plastic deformation (SPD) techniques, has been developed. SPD enables to manufacture high-strength bulk billets out of metallic materials [11]. One of the SPD techniques is equal channel angular pressing (ECAP) [12], effected in several cycles of deformation. The principle of this ECAP strength enhancement technique is the maximum refinement of the grain structure to the sizes of submicrocrystalline- and nano-scale [13].

The SPD techniques considerably enlarge the field of application of such relatively cheap alloys as low-carbon steels. Therefore, complex comparative tribological investigations of low-carbon steel in various structural and phase

conditions after heat and SPD treatments are of great research and practical interest.

2. MATERIAL AND METHODS OF INVESTIGATION

Low-carbon steel with the carbon content of up to 0.2% (percent by weight) was employed as material for present study. Samples after hot-rolling were taken as the initial condition. The dimensions of the samples are of 20 mm in diameter and of 100 mm in length.

In order to transform the investigated steel into the equilibrium condition and to release residual stresses, comprising quenching in water from the temperature of 880° C with a subsequent tempering at the temperature of 600° C and holding in a furnace at that temperature for 1.5 hour, was performed.

The ECAP scheme [14] shown in Fig. 1 was chosen for strain hardening of the initial material by SPD technique. ECAP was performed on a die-set with the angle of channel intersection of 120° at a temperature of 400° C, and with rotation of the billet along its longitudinal axis by 90° after every cycle. The number of deformation cycles was four.

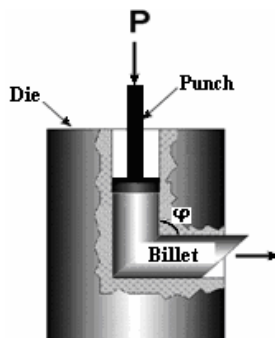


Figure 1. Scheme of a SPD technique – equal-channel angular pressing (ECAP).

The accumulated strain degree was calculated by the following formula [15, 16]:

$$\varepsilon = N \frac{2 \cot(\varphi / 2)}{\sqrt{3}}, \quad (1)$$

where ε is accumulated strain degree; N is the number of deformation cycles; φ is the angle of channel intersection.

The microstructure investigations were conducted with the help of optical metallography at different magnifications. The grain sizes were calculated by a secant line technique [17].

The techniques of evaluation of adhesive bond shear strength τ_n , determination of the adhesive component of the friction coefficient f_a [18] (Fig. 2, a) and evaluation of the friction coefficient f and wear rate J according to the scheme «block - on -

disc» were employed for tribological studies [19] (Fig. 2, b).

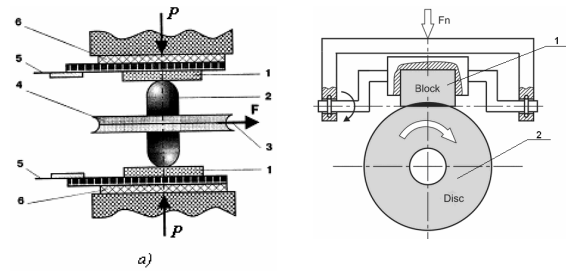


Figure 2. Schemes for tribological investigations: a) 1 - tested samples; 2 - spherical indenter; 3 – cable; 4 – disk groove; 5 – current conductor line; 6 – electrical insulating spacer [18]; b) 1 – tested sample; 2 – rotating steel disk.

The samples for evaluation of adhesive bond shear strength and determination of the adhesive component of the friction coefficient were prepared in the shape of discs of 20 mm in diameter and 5 mm in thickness and the spherical indenter with the sphere radius of 2.5 mm out of tool high-cutting steel $Fe - 6W - 5Mo$. Tests on determination of the adhesive bond shear strength were carried out at 20, 200 and 400° C on a one-ball adhesiometer according to the scheme presented in Fig. 2, a [18]. The initial roughness of the contact surfaces of the samples for the test and the indenter were within 0.06 – 0.16 μm Ra.

The adhesive bond shear strength (τ_n) (MPa) was calculated with the help of the formula [18]:

$$\tau_n = 0.75 \times \frac{M}{\pi \left(\frac{d_{1,2}}{2} \right)^3}, \quad (2)$$

where τ_n is adhesive bond shear strength, MPa; $d_{1,2}$ are the diameters of the prints on the samples under investigation, mm; M – the indenter rotary moment, N*mm.

The adhesive component of the friction coefficient was calculated according to the following formula:

$$f_a = \frac{\tau_n}{p_r}, \quad (3)$$

where f_a is adhesive component of the friction coefficient; p_r – the normal pressure, MPa, and

$$p_r = \frac{P}{\pi \cdot \left(\frac{d_{1,2}}{2} \right)^2}, \quad (4)$$

where P – the compression force, N. $P = \text{Const} = 2400$ N for present test.

The samples in the shape of cubic blocks with the face of 12.7 mm were used for tests on the scheme «block-on-disc» (Fig. 2, b). The discs of 70 mm in diameter and with a thickness of 20 mm

were prepared from tool high-cutting steel $Fe - 6W - 5Mo$. Three identical disks in accordance with numerous samples were prepared for testing. The initial roughness of the blocks and discs was in the range of $0.06 - 0.16 \mu m$ Ra. During testing the temperature of the tested sample was measured and variations of the temperature were recorded. The tests were carried out at room temperature on the tribometer *Timken* at a disc rotating speed of 1000rpm and a normal load of 5N for 15 min. The slide distance comprised 330000 cm. Every sample was weighed before and after testing in order to determine the wear rate. The geometric contact area was determined after testing. Then the wear rate was calculated according to the formula:

$$J = Q/qS_cL, \quad (5)$$

where J is wear rate value; Q – loss of weight, g ; q – the material density, g/cm^3 ; S_c – the contact geometric area, cm^2 ; L – the slip distance, cm .

The wear of the discs fabricated from the tool high-cutting steel $Fe - 6W - 5Mo$ and quenched to the hardness of HRC 58-65 was not taken into consideration due to its small value compared to the wear of the samples under testing.

The scanning electron microscope (SEM, Hitachi-S3500) with the add-on unit for Energy Dispersive Spectrometer (EDS) was used to conduct chemical analysis of the worn surface of the samples. The microhardness $H\mu$ was measured on the *Micromet-5101* at a load of 1.96 N with a holding of 15 sec.

Table 1. Surface analysis of steel 20 in various structural conditions

Treatment	Mean grain size, μm	Microhardness, MPA		Oxygen content, wt %	
		Before tests	After tests	Before tests	After tests
Hot-rolled (initial)	70	241	283	1.31	1.73
Heat treatment	50	265	307	1.51	1.82
Heat treatment + Severe Plastic Deformation (4 ECAP passes)	0.5	319	352	3.42	3.64

The microhardness measurement and the chemical analysis of the wearing surface with respect to the oxygen content were performed before and after the tests.

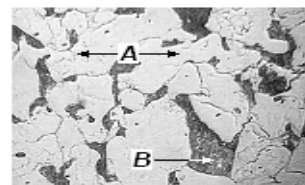
3. THE INVESTIGATION RESULTS

3.1 Measurement of microhardness and oxygen content of the sample surface

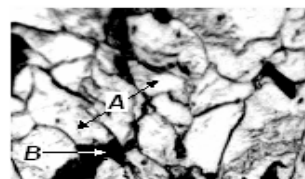
On the basis of microhardness measurement and the chemical analysis of the worn surfaces with

respect to the oxygen content, it was found that after tribological tests the microhardness of worn surfaces and the oxygen content of samples increase (referring to Table 1). Table 1 shows that the lowest values of the investigated parameters correspond to the initial (hot-rolled) condition of the material, and the highest values correspond to the condition of the material subjected to heat-treatment with subsequent severe plastic deformation by the ECAP technique.

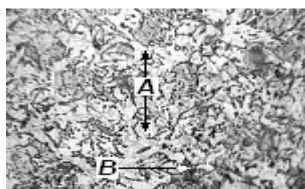
As seen from the table 1, the material's structural condition influences significantly the increase of microhardness and oxygen content on the surface of the low-carbon steel. Namely, the smaller is the mean grain size, the higher are the mentioned parameters. The material under consideration relates to hypoeutectoid steels, which possesses two structure components: ferrite and granular pearlite. The initial (hot-rolled) condition represents a coarse-grained ferrite-pearlite mixture (Fig. 3, *a*: ferrite – light grains, pearlite and carbide particles – dark grains). After heat-treatment (quenching after heating up to $880^\circ C$ and subsequent tempering at $600^\circ C$) decrease of the initial carbide inhomogeneity and a certain mean grain size reduction were observed (Fig. 3*b*). After cyclic SPD by the ECAP technique the carbide phase is partially spheroidized, and areas in the shape of carbide net, decorating the boundaries of the ferrite grains, can be observed (Fig. 3, *c*)



a – in the initial condition, the mean grain size of $70 \mu m$ (x 500);



b – after heat-treatment, the mean grain size of $50 \mu m$ (x 500);



c – after heat-treatment and 4 ECAP passes, the mean grain size of $0.5 \mu m$ (x 1000).

Figure 3. Steel 20 microstructure: A – ferrite; B – pearlite. In fig. 3, *c* pearlite is represented in the form of net on the boundaries of ferrite grains.

Fig. 4 represents surfaces of samples with different types of treatment before tribological tests. The surface areas, which were subjected to spectrographic analysis, are marked by rectangles

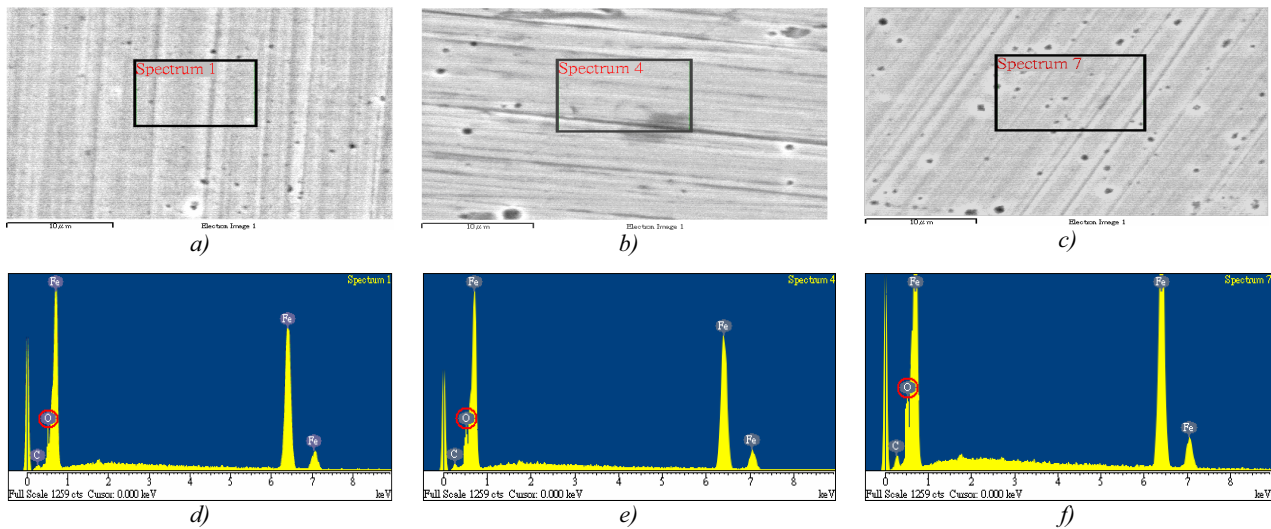


Figure 4. Surfaces of samples with different types of treatment before tribological tests: *a)* – in the initial condition, the mean grain size of 70 μm ; *b)* – after heat-treatment, the mean grain size of 50 μm ; *c)* – after heat-treatment and 4 ECAP passes, the mean grain size of 0.5 μm ; SEM - EDS spectrum: *d)* - in the initial condition; *e)* - after heat-treatment; *f)* - after heat-treatment and 4 ECAP passes. On the spectra there are displayed and marked oxygen peaks, corresponding to its content on the surface.

From the analysis of the obtained spectra it is observed that the biggest amount of oxygen in the form of oxides is revealed on the surface of the sample after heat-treatment and 4 ECAP passes (Fig. 4, *f*). Analogous spectra were obtained also on samples after performance of tribological tests.

It is known that severe plastic deformation, leading to grain structure refinement, is accompanied by increase of defect density and activation energy both inside the material and on its surface [13]. Moreover, in work [13] it is noted that there is an increase of diffusion rate in ultrafine-grained (UFG) materials, which contribute to energy reduction. Thus, we suppose that on the surface of UFG materials oxides are formed more intensively due to a higher diffusion rate of chemical elements from the environment, in particular, oxygen.

Analogous studies were performed on a magnesium AZ91D alloy [20] and on commercially pure titanium [21]. In all likelihood it is the common property of ultrafine grained (UFG) and nanostructured materials, grain boundaries of which contribute to a more active adsorption of oxygen on a metal surface with forming compounds with alloy components in the form of oxides. The numerical values of the oxygen content on the sample surface before and after tribological tests are shown in Table 1. It should be noted that after the tribological tests the oxygen content in the surface of all the samples increased as compared to the results obtained before the tests. These data associate with the results of other researchers [6, 10, 22 and others], and can be explained by the micro-structural changes on the surface under the

action of normal pressures, friction forces and friction heating.

3.2 Tribological investigations according to the scheme “block-on-disc”

Fig. 5 represents characteristic areas of the worn surfaces on samples of low-carbon steel after different types of treatment with different microstructure.

Fig. 5 indicates that the worn surfaces in all the cases represent a combination of a metallic matrix in the form of a ferrite-pearlite mixture and oxides in different proportions, which depends on the type of treatment. Referring to table 1 and Fig. 4, *c*, it was found that on the worn surface of a sample with an ultrafine-grained structure after SPD by the ECAP technique there is a bigger amount of oxygen in the form of fine-dispersed oxides with mostly the same amount of iron and carbon compounds in the form of pearlites (Fig. 5, *c*). Contact interaction of the sample in the initial (hot-rolled) condition (Fig. 5, *a*) under the assumed test conditions, is accompanied by a more intensive adhering due to a less amount of oxides. Intensive adhering activates formation of adhesive bonds between the rotating disk made of tool steel and soft ferrite component. Subsequently, the failure of these bonds occurs under the action of friction forces. The pearlite phase with an increased carbon content (represented as dark parts in the photos) is located in the form of large fragments on the surface. After heat-treatment of steel samples (Fig. 5, *b*) pearlite agglomeration fragments of a smaller size are observed, but it does not have a considerable influence on friction forces

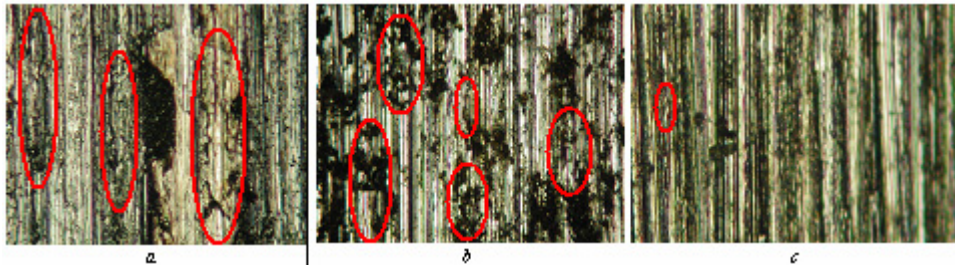


Figure 5. Worn surface on low-carbon steel after various types of treatment: *a* – sample in the initial condition (hot-rolled); *b* – samples after heat treatment (quenching and tempering); *c* – sample after ECAP and preceding heat treatment, x100.

Moreover it has been established that depending on the structure condition of low-carbon steel, and, consequently on the oxygen concentration on the surface there is observed different character of wearing in the contact zone. In Fig. 5, the areas of surface, where in the course of friction traces of spalling and pitting were observed, are marked. It can be observed in Fig. 5, *c*, the sample, subjected to ECAP processing has only a small area with spalling traces, while samples in the initial condition and after heat-treatment have more such areas, and they are roughly equal in their total surface area. However this fact requires further special inspection and investigation, as it is the basis for understanding the wear mechanism in low-carbon steels with different microstructure.

During the tribological testing the friction pair “low-carbon steel – tool steel” according to the scheme “block-on-disc” various characters of the friction coefficient changing with time were revealed in Fig. 6.

Severe plastic deformation by the ECAP technique leads to dispersion and a more uniform distribution of pearlite particles (Fig. 5, *c*), and also to hardening of the material due to structural constituents refinement.

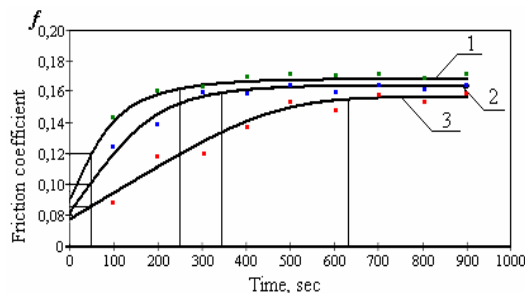


Figure 6. Dependence of the friction coefficient on testing time for the friction pair «low-carbon steel – tool steel $Fe - 6W - 5Mo$ »: 1 – initial material (coarse-grained hot-rolled); 2 – material subjected to heat-treatment; 3 – material with ultrafine-grained structure after heat-treatment and SPD processing by ECAP technique.

Fig. 6 shows that the material with the ultrafine-grained structure after being subjected to heat treatment with subsequent severe plastic

deformation (SPD) by ECAP technique has the lowest friction coefficient in the analyzed friction pair. Probably, friction conditions become more favorable due to the increase of strength and hardness of the low-carbon steel, and also to the uniform distribution of pearlite particles and larger oxygen content in the form of oxides and carbide particles on the surface. Such friction conditions, to an extent, can be compared to friction in a friction bearing [23]. As a result, the total value of the friction coefficient decreases. Thus we observe a complex formation of a “third body” [24], which consists of oxides, fine dispersion particles of pearlite and carbides. Besides, this wear test provides smoother transition to the established mode of friction that contributes to decrease of the wear rate. The bar chart in Fig. 7 shows the results of wear rate.

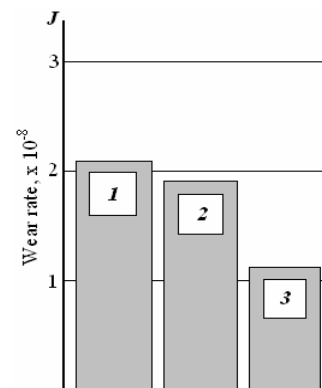


Figure 7. Wear rate of low-carbon steel depending on the structural condition of the material under investigation: 1 – initial material (coarse-grained hot-rolled); 2 – material subjected to heat-treatment; 3 – material with ultrafine-grained structure after heat-treatment and SPD processing by ECAP technique.

3.3 Adhesive bond shear strength evaluation

Fig. 8 shows the results of the tribological tests on determination of the adhesive bond shear strength τ_n depending on the pressure p_r during friction contact at various temperatures. These investigations proved the linear character of the

dependence $\tau_n = f(p_r)$ both under the conditions of an elastic contact and plastic deformation at different temperatures θ . From these dependencies it follows that the adhesive component of the friction coefficient (f_a), which is calculated from the formula (3), increases with the growth of the temperature. The value f_a is calculated as a tangent of the angle of slope to the x-axis (i.e. a relation of adhesive bond shear strength (τ_n) to a normal pressure (p_r)).

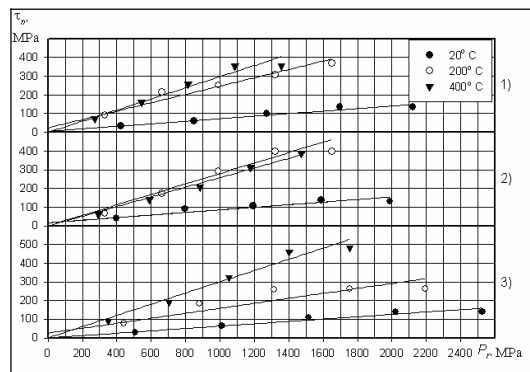


Figure 8. Dependence of the adhesive bond shear strength on the normal load in the tribological pair “low-carbon steel-tool steel $Fe - 6W - 5Mo$ at various temperatures and during various treatment of the material under investigation: 1 – initial material (coarse-grained hot-rolled); 2 – material subjected to heat-treatment; 3 – material with ultrafine-grained structure after heat-treatment and SPD processing by ECAP technique.

The obtained temperature dependence of the adhesive component of the friction coefficient f_a for the friction pair under investigation is shown in Fig. 9. The curves in Fig. 9 are, plotted as a result of processing of data, represented in Fig. 8 and after calculation of f_a .

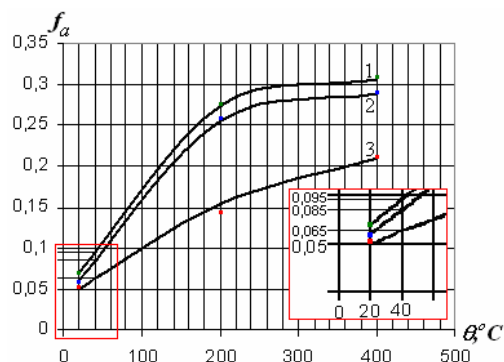


Figure 9. Changes in the adhesive component of the friction coefficient depending on the temperature: 1 – initial material (coarse-grained hot-rolled); 2 – material subjected to heat-treatment; 3 – material with ultrafine-grained structure after heat-treatment and SPD processing by ECAP technique. The right bottom corner represents a magnified and horizontally strained graph segment.

Fig. 8 and 9 show experimental dependencies of adhesion interaction parameters on pressure and temperature, which were typical of heavy loaded tribological pairs, and also of a contact of tool and treated material under conditions of mechanical treatment.

It has been found that the increase of adhesive bond strength is accompanied by the growth of normal pressure p_r on the contact. The best effect of abovementioned increase is observed in the samples with UFG structure after ECAP, which is probably connected with a more intense hardening of material due to deformation treatment in comparison to the other two conditions of the materials. It is known that with the increase of the temperature the bearing capacity of the contact gradually decreases [18]; as a result the adhesive component of the friction coefficient f_a increases (see Fig. 9).

However in the represented dependencies, it is seen that in low-carbon steel samples, subjected to heat treatment with a subsequent SPD by the ECAP technique, the adhesive component values of the friction coefficient are considerably lower within the whole investigated temperature range, comparing with the two other conditions. Data obtained for the initial sample and for the sample after heat treatment (without a subsequent SPD) do not differ significantly both by value and the character of the f_a variation. Probably it is predetermined by a slight difference of the mean grain size of the samples existing between the initial and heat treated conditions, and also by a very close oxygen content exhibiting within both materials of those conditions (see the Table 1). On the basis of the above mentioned suggestion, we suppose that the adhesive component of the friction coefficient f_a is directly connected with the structural condition of surface and with the oxygen content, because the oxide films (possessing high hardness) prevent the sample from a direct contact with the disc in one case, and from spherical indenter in another case.

3.4 Comparative evaluation of tribological investigation results of the two alternative techniques

Comparing the results given in Fig. 6 and Fig. 9, it can be noted that they are similar in the uprising area (left part of the graphs), and it can be supposed that the greatest contribution to the general changes in that integral value of the friction coefficient is introduced by its adhesive component. Probably it is connected with the low-carbon steels' tendency for strain hardening via structural grain refinement. A more flat area on the curve, corresponding to the

investigated sample with a UFG structure after SPD treatment by ECAP technique, verifies that the sample has higher surface bearing capacity, but at the same time, this sample requires more time for wearing-in.

From the of temperature variation dynamics during temperature measurement in the process of tests of the block-on-disc scheme, it has been established that the maximum heating of the sample with the adopted conditions of test and dimensions of the samples and disks was at about $40 \pm 1.5-2.0^\circ\text{C}$. This temperature was achieved 50 seconds after the start of the tribological testing and practically did not change from then until the end of the tests.

In accordance with the known mechanical attraction friction theory [24] the integral friction coefficient value (f) is formed from the deformation (f_d) and adhesive (f_a) components. The deformation component of the friction coefficient is formed by resistance forces of the straining “bulge”, moving ahead of the irregularities intruded into the surface of a softer one of the contacting and slipping in relation to one another bodies. The value of the deformation component of the friction coefficient f_d depends on the number of intruded irregularities and their relative intrusion, which can be determined analytically [25] or experimentally as:

$$f_d = f - f_a \quad (5)$$

In order to compare the results of the investigations, represented in Fig. 6 and Fig. 9 a data cut-off, corresponding to the period of stabilization of the friction heating temperature (50 sec.) and the maximum value of the temperature after 50 sec (40C°) was made in Fig. 6 with the following extrapolation of these data on curves, represented in Fig. 9. With the help of formula (5) the deformation component of the friction coefficient has been calculated.

Values of the total friction coefficient (f) and its adhesive component (f_a), obtained in comparable conditions on the basis of experimental data and represented in Fig. 6 and 9, showed that the deformation component (f_d) values are in the range $0.020 \pm 10\%$ regardless of the type of treatment and the structural condition of the samples. Thus it can be concluded that in the adopted testing conditions it is the adhesive component that has the biggest influence on the friction coefficient (f).

4. CONCLUSIONS

1. Severe plastic deformation by equal channel angular pressing technique was shown to enhance efficiently the strength of the low-carbon steel due to its grain structural refinement that considerably

influences the decrease in the friction coefficient and its adhesive component;

2. The increased oxygen content on the material surface after SPD compared to both initial condition and after heat-treatment contributes to stronger passivation of the surface due to the formation of oxide films, which together with strain hardening contributes to decrease in the friction coefficient in the specified temperature range and increase in wear resistance as well;

3. The surface of the investigated material after SPD treatment by the ECAP technique possesses a higher bearing capacity and requires more time for wearing-in in friction assemblies;

4. Oxygen content increase in the form of metal oxides on the surface of low-carbon steels is accompanied by an increase of the deformation component of friction coefficient.

5. The present wear mechanism of low-carbon steel with heat-treatment and processing by ECAP against tool steel $Fe - 6W - 5Mo$ is suggested as the adhesive types

ACKNOWLEDGEMENTS

The authors express gratitude to Dr. S.V. Chertovskikh (Ufa State Aviation Technical University, Russia) and Prof. S.-G. Hwang (National University Formosa, Taiwan) for active participation in tribological investigations and processing of results.

The work was carried out within the frames of the joint Russian-Taiwan project No 07-08-92001 HHC_a, supported by RFBR, jointed with project NSC 96-2923-E-194 -001 -MY3 by NSC of Taiwan.

REFERENCES

- [1] A.V. Chichinadze, E.M. Berliner, E.D. Brown et al., Friction, wear and lubrication (tribology and triboengineering), Mashinostroenie, Moscow, 2003
- [2] Shabashov V.A., Korshunov L.G., Mukoseev A.G. et al. Deformation-induced phase transitions in a high-carbon steel // Materials Science and Engineering, 2003. Vol. A346. P. 196-197.
- [3] Garnham J.E., Beynon J.H. Dry rolling-sliding wear of bainitic and pearlitic steels//Wear, 1992. Vol. 157, № 1. P. 81-109.
- [4] G.S. Fox-Rabinovich, G.C. Weatherly, A.J. Kovalev, L.Sh. Shuster and others Nano-Crystalline FAD (Filtered Arc Deposited) TiAlN PVD Coatings for High-Speed Machining Application//Intern. Conf. on Metallurgical Coatings and Thin Films. Progr. and abst. – San Diego, California, April 28 – May 2, 2003, p. 52.
- [5] Luzhnov Yu.M. and others. The Efficiency of the Friction of the “wheel-rail” – System/New Achievements in Tribology. 6th Intern. Symp.

- “Insycont-02”, September 2002, Krakow: Poland. P. 129-135.
- [6] Johnson K.L. Contact Mechanics. Cambridge University Press, 1987. 452 p.
- [7] L.G. Odintsov, Strengthening and finishing of parts via surface plastic deformation: Reference book, Mashinostroenie, Moscow, 1987.
- [8] Yang Z.Y., Naylor M.G.S., and Rigney DA. Sliding wear of 304 and 310 stainless steels//Wear. 1985. Vol. 105. P. 73—86.
- [9] Hornbogen E. Microstructure and Wear. — Metallurgical aspects of wear. — Bad Pymont, 1979. P. 23-49.
- [10] Perez-Unzueta A. J, Beynon J. H. Microstructure and wear resistance of pearlitic rail steels//Wear, 1993. Vol. 162-164. P. 173-182.
- [11] R.Z. Valiev The new trends in fabrication of bulk nanostructured materials by SPD processing, J. Mater. Sci., Vol. 42 (2007), pp. 1483-1490.
- [12] G.I. Raab, F.F. Safin, T.C. Lowe, Y.T. Zhu, R.Z. Valiev Development of ECAP-Conform to Produce Ultrafine-Grained Aluminum, Proc. of Ultrafine Grained Materials IV symposium held during the TMS 2006 Annual Meeting in San Antonio, Texas, USA, March 12-16, 2006, eds. Y. Zhu, T. Langdon, Z. Horita, M. Zehetbauer, S.L. Semiatin, T. Lowe (2006) pp. 171-177.
- [13] R.Z. Valiev, T.G. Langdon Principles of equal-channel angular pressing as a processing tool for grain refinement, Progress in Materials Science, Vol. 51 (2006), pp. 881-981.
- [14] R.Z. Valiev, Y. Estrin, Z. Horita, T.G. Langdon, M.J. Zehetbauer, Y.T. Zhu, Producing bulk ultrafine-grained materials by severe plastic deformation, J. Mater. 58 (2006) 33.
- [15] V.M. Segal, V.I. Reznikov, A.E. Drobyshevskii, V.I. Kopylov et al., Plastic processing of metals by simple shear, Izvestia AN USSR Metals. 1 (1981) 115-123.
- [16] Segal V.M. Equal channel angular extrusion: from macromechanics to structure formation //Mater. Sci. Eng. 1999. (A271). P. 322-333.
- [17] S.A. Saltykov Stereometric Metallographic. Metallurgy, Moscow, 1976.
- [18] V.V. Stolyarov, L.Sh. Shuster, M.Sh. Migranov, R.Z. Valiev, Y.T. Zhu Reduction of friction coefficient of ultrafine-grained CP titanium//Materials Science and Engineering A371, 2004. pp 313-317.
- [19] Chichinadze A.V. Evolution Method of the Carbon Friction Composite Materials Used in Multiple Disk Aviation Brakes//Tribologia. Warszawa. No. 1. 2000. Part I. P. 7-22; No. 2. 2000. Part II. P. 133-154; No. 1. 2001. Part III. P. 23-38.
- [20] V.I. Semenov, Y.-R. Jeng, S.-J. Huang, Y.-Zh. Dao, S.-J. Hwang, L. Sh. Shuster, S. V. Chertovskikh, P.-Ch. Lin, Tribological properties of the AZ91D magnesium alloy, hardened with silicone carbide and by severe plastic deformation, J. of Fri. and Wear. 30 (2009) 194-198.
- [21] V.V. Stolyarov, L.Sh. Shuster, S.V. Chertovskikh Tribological behaviors of ultrafine-grained titanium alloys// Friction and lubrication in machines and mechanisms.-2006.-№10. — p. 11-19.
- [22] A.S. Akhmatov, Molecular physics of boundary friction, State publishing House of physico-matematical literature, Moscow, 1963.
- [23] Semenov A.P., Antifriction and antiseizure sliding bearings, Proc. III Int. Symposium of tribo-fatigue ISTF 2000, Beijing China Human University Press, China, (2000) 629-632.
- [24] I.V. Kragelskii. Friction and wear. Mashinostroenie. Moscow, 1968.
- [25] I.V. Kragelskii, M.N. Dobyichin, V.S. Kombalov. Principles of friction and wear calculations. Mashinostroenie, Moscow, 1977.